

## Geochemistry of dark coastal heavy-mineral beaches sand (Annaba, Northeast Algeria)

### Géochimie des sables sombres côtiers à minéraux lourds (Annaba, Nord-Est Algérien)

Asma Chemam<sup>1\*</sup>, Soraya Hadj Zobir<sup>2</sup>, Menana Daif<sup>1</sup>, Uwe Altenberger<sup>3</sup> & Christina Günter<sup>3</sup>

<sup>1</sup> Badji-Mokhtar/Annaba University, Laboratory of LGRN, P.O. Box 12, 23000, Annaba, Algeria.

<sup>2</sup> Badji-Mokhtar/Annaba University, Laboratory of Soils and Sustainable Development, P.O. Box 12, 23000, Annaba, Algeria.

<sup>3</sup> Institute of Earth and Environmental Science, University of Potsdam, Karl-Liebknecht-Strasse 24-25, D 14476 Potsdam-Golm Germany.

Soumis le : 06/03/2017

Révisé le : 19/09/2017

Accepté le : 26/09/2017

#### ملخص

تتضمن منطقة الدراسة (عين عشير والشاطئ العسكري) إلى كتلة الإيدوغ الجبلية/عصابة الجزائر. ميزنا في شاطئ عين عشير رمالا بنية فاتحة ورمالا فاتحة تميل إلى اللون الأحمر. تظهر هذه الأخيرة بعد عاصفة بحرية. أما رمال الشاطئ العسكري فهي ذات لون قاتم دائما. تكونت رمال عين عشير والشاطئ العسكري من الميكاشيبست ذي الغرانات والسترووليت والميكاشيبست ذي الأندلوسيت أو النيستان، المرمر، السكارن ذي الإبيدوت، المغماتيت وعروق المرور الصفاحي ذي التورمالين. تم تحليل رمال الشاطئين إلى عناصر رئيسية و ثانوية إضافة إلى التراب النادر. بينت تحاليل الرمال الفاتحة وكذلك القاتمة لعين عشير اختلافات هامة في تركيبهما الكيميائي. تركزت بعض العناصر الأساسية والثانوية وكذلك في التراب النادر في الرمال الفاتحة هي أقل من الرمال القاتمة. وبالمقابل فإن التركيب الكيميائي للرمال القاتمة للشاطئين متماثل. بينت هذه الدراسة وجود روابط إيجابية بين محتوى العناصر الرئيسية، الثانوية، التراب النادر والتركيز المتميز للفلزات الثقيلة خاصة مع وجود فلزات التحول مثل الغرانات، سترووليت، التورمالين والإبيدوت.

**الكلمات المفتاحية:** فلزات ثقيلة - عناصر رئيسية - عناصر ثانوية - رمال الشاطئ.

#### Résumé

La région étudiée (Ain Achir et Plage-Militaire) fait partie du Massif de l'Edough/Annaba/Algérie. A Ain Achir on distingue du sable brun clair et du sable sombre rougeâtre. Ce dernier apparaît principalement après une tempête de mer. Celui de la Plage-Militaire est de couleur sombre en permanence. Les sables étudiés se sont formés près des micaschistes à grenat -, staurolite - et/ou à andalousite ou disthène, des marbres, des skarns à épidote, des migmatites et des veines du quartzo-feldspathiques à tourmaline. Le sable des deux plages a été analysé en éléments majeurs, en traces, ainsi qu'en terres rares. Le sable clair et celui sombre de la plage de Ain Achir montrent d'importantes différences dans leurs composition chimiques. Les concentrations de certains majeurs, traces et Terre Rares dans le sable clair sont inférieures à celles du sable sombre. Par-contre la composition chimique des sables sombres des deux plages est similaire. Cette étude montre une forte corrélation positive entre la teneur en éléments majeurs, traces, terres rares et la concentration modale en minéraux lourds et particulièrement avec les minéraux du métamorphisme tels que le grenat, la staurolite, la tourmaline et l'épidote.

**Mots clés :** Minéraux lourds- élément majeur –élément trace – les terres rares- sable de plage.

#### Abstract

The study area (Ain Achir and Plage-Militaire beaches) is a part of the Edough Massif/Annaba /Algeria. Recent beach sediments of Ain Achir are characterized by light sand and dark reddish one. This latter appears mostly after a sea storm. The Plage-Militaire sands are permanently dark brown. The study sands are formed near to garnet-, staurolite- and/or andalusite-, kyanite- micaschists, marble, epidotic skarns, migmatites and numerous tourmaline bearing quartzo-feldspathic veins. Whole sand samples from the two beaches have been analyzed in major and trace elements, including rare earth elements (REE). At Ain Achir beach, the light sand and the dark one show significant differences in their chemical compositions. Some of the major elements, the trace elements as well as the Rare Earth Elements in the light sand are lower than in the dark sand samples. Whereas the chemical composition of the dark sand of the two beaches are nearly similar. This study shows a strong positive correlation between the concentration of major, traces and REE elements and the amount of heavy and especially metamorphic minerals like garnet, staurolite, tourmaline and epidote.

**Key words:** Heavy minerals- Major - Trace element – REE- Sand-Beach

\* Corresponding Author: Chemam.asma@gmail.com

## 1. INTRODUCTION

The majority of the heavy mineral sand-beaches in the world occur as deposits in the swash zone of the coastal sediments. The present paper presents the first study of heavy mineral sands from the Annaba/Algeria coastal sands. The Annaba coastline is composed of a dozen of fine sand beaches. Some beaches are characterized by a red-brownish sand colour, the Ain Achir and the Plage-Militaire beaches are one of them. These two beaches are located along the Northern coast of Annaba/Algeria. The Ain Achir sand is light and mostly dark brown after a sea storm, whereas the Plage-Militaire sand is permanently dark brown. The mineralogical composition of the brown sand of these two beaches is dominated by heavy transparent minerals such as: garnet, staurolite, kyanite, tourmaline and epidote. The sand is also characterized by anomalously high concentrations of some major (e.g.  $TiO_2$ ,  $MgO$ , and  $Fe_2O_3$ ), trace and rare-earth elements. The objective of this paper is to identify the relationships between the observed heavy minerals in these two beaches and selected major, trace and rare earth elements.

## 2. STUDY AREA

The study area "Ain Achir and Plage-Militaire" beaches is located at the Cap de Garde between  $36^{\circ} 57'20'' - 36^{\circ} 57'54''$  latitude and  $7^{\circ} 46'76'' - 7^{\circ} 46'96''$  longitude (Fig.1a).

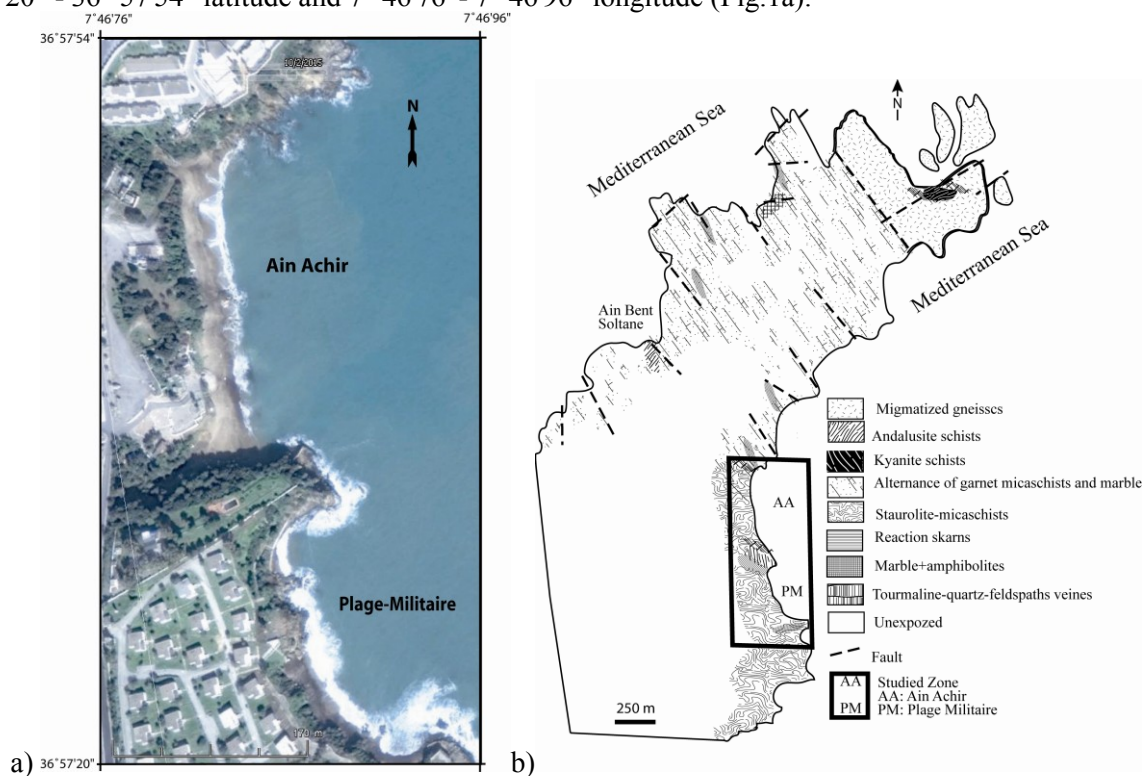


Figure.1. a) Google Earth view of the Ain Achir and the Plage-Militaire beaches, b) Simplified geological maps of the Cap de Garde with the study beaches' location, [2, 4, 7]

The Cap de Garde is the north part Edough Massif/Annaba/Algeria and extends over a distance of about 3 km in length. The study area is composed by two small beaches: Ain Achir (275x30m) and Plage-Militaire (236x20m) (Fig.1a). These two beaches are underlined by metamorphic rocks (Fig.1b): Andalusite-garnet-schists, kyanite-schists, staurolite-garnet-schists alternating with marble layers, quartzite and numerous tourmaline-quartz-feldspaths veins and some garnetites layers which are considered as metamorphosed paleo-garnet beach-sand placer [1]. The contact between the staurolite-garnet-schists and the marble layers is underlined by reaction skarns (epidote rich skarns). The North part of the Cap de Garde is composed by migmatized gneisses and outcrops of massif marbles with some locally metamorphosed submarine basic ashes layers [2]. The Cap de Garde and the Edough Massif have experienced the same polyphase regional metamorphism characterised by high-pressure (12–14 kbar) and medium-temperature metamorphic conditions (500-600 °C) [3, 4, 5, 6, 7]. The different metamorphic units undergone a first oblique deformation characterized by syn-metamorphic

folds followed by flexural shear generating upright folds of N140° direction, anticlines with direction N50° to N60° and shear senses of N120° to N160° direction.

### 3. ANALYTICAL METHODS AND SAMPLING

Thirty-five (18 at Ain Achir and 17 at Plage-Militaire beach) superficial hand samples with a single weight of 3kg were acquired from a 10x15m grid covering the two beaches. The bulk sample was reduced by coning and quartering and a 100-g portion of the sample was selected for laboratory analysis [8]. Analyses for major and minor elements and for some trace elements have been conducted on fused glass and have been pressed powder disks respectively. Major, minor and some trace elements have been acquired by a Siemens SRS303-AS XRF with a Rh X-ray tube at standard running conditions at the GeoForschungs Zentrum Potsdam (GFZ), Germany. Measurements of trace elements, including Nb, have been performed in the ICP-MS laboratory at the (GFZ), using a VG Elemental Plasma Quad System PQ2+i. REE were analyzed at the GFZ laboratories by an ICP-OES (Varian Vista MPX) after separation of major and most trace elements. Whole heavy mineral grains were identified under incident light using a binocular microscope. Random grain samples were also mounted in thin section for identification using a petrography microscope, thus providing a means of verifying the bulk identifications achieved under incident light. The minerals registered by microscopic investigations were further checked by X-ray. Counts of minerals were made under the microscope. The occurrence of clays has been determined using the methyl-blue method. Correlation and factor analysis were performed for traces and rare earth elements using the software XLSTAT-PRO 7.5.

## 4. RESULTS

### 4.1. Sand mineralogy

The Ain Achir and the Plage-Militaire sand show meaningful differences in their mineral proportions, the results are shown in table 1a and 1b and figure 2. Ain Achir sand shows two kinds of colours: light sand which is composed by an average of 40% of heavy minerals and dark sand which is composed by an average of 77% of heavy minerals. The average compositional framework of the black sand consists of staurolite (45%) as main mineral, followed by garnet (20%), tourmaline (9%), kyanite and epidote (2%). The Plage-Militaire is characterized by higher average in heavy mineral content (93%). As in the Ain Achir sand, the staurolite is the main mineral (46%) followed by the garnet (31%). Tourmaline is more present (13%) than in Ain Achir sand whereas kyanite and epidote are low (2 and 1% respectively).

Table 1. Mineral contents in percentage of the heavy and light minerals: a) at Ain Achir sand beach, b) at the Plage-Militaire. Ep: epidote, Grt: garnet, Ky: kyanite, St: staurolite, Tur: tourmaline, Qz: Quartz, Cal: calcite, [9].

|    |                 | Samples | Grt | St | Ky | Tur | Ep | Qz | Cal | ΣHM% | ΣLM% |    |
|----|-----------------|---------|-----|----|----|-----|----|----|-----|------|------|----|
| a) | LIGHT SAND (LS) | AA1a    | 4   | 10 | 4  | 8   | 9  | 7  | 57  | 36   | 64   |    |
|    |                 | AA1b    | 7   | 36 | 5  | 4   | 0  | 10 | 38  | 52   | 48   |    |
|    |                 | AA2b    | 5   | 10 | 4  | 4   | 3  | 14 | 59  | 27   | 73   |    |
|    |                 | AA4a    | 10  | 31 | 4  | 5   | 1  | 10 | 37  | 52   | 48   |    |
|    |                 | AA4b    | 6   | 26 | 3  | 1   | 2  | 18 | 43  | 39   | 61   |    |
|    |                 | AA5a    | 11  | 25 | 6  | 7   | 0  | 11 | 41  | 48   | 52   |    |
|    |                 | AA5b    | 7   | 10 | 10 | 7   | 0  | 11 | 54  | 35   | 65   |    |
|    |                 | AA5c    | 11  | 9  | 2  | 4   | 0  | 20 | 54  | 26   | 74   |    |
|    |                 | AAGa    | 13  | 24 | 2  | 8   | 2  | 16 | 35  | 49   | 51   |    |
|    | DARK SAND (DS)  | AACa    | 25  | 43 | 0  | 16  | 5  | 2  | 9   | 89   | 11   |    |
|    |                 | AA2a    | 17  | 48 | 1  | 6   | 3  | 2  | 23  | 75   | 25   |    |
|    |                 | AA2c    | 15  | 33 | 5  | 15  | 3  | 8  | 21  | 70   | 30   |    |
|    |                 | AAMa    | 15  | 44 | 1  | 6   | 0  | 10 | 24  | 66   | 34   |    |
|    |                 | AAMb    | 23  | 67 | 0  | 3   | 2  | 1  | 3   | 96   | 4    |    |
|    |                 | AA3a    | 11  | 43 | 0  | 8   | 3  | 8  | 28  | 64   | 36   |    |
|    |                 | AA3b    | 18  | 40 | 1  | 6   | 0  | 9  | 26  | 65   | 35   |    |
|    |                 | AA3c    | 13  | 44 | 6  | 9   | 0  | 6  | 22  | 72   | 28   |    |
|    |                 | AAGb    | 39  | 40 | 0  | 15  | 1  | 0  | 5   | 95   | 5    |    |
|    | Average %HM LS  |         |     | 8  | 20 | 4   | 5  | 2  | 13  | 47   | 40   | 60 |
|    | Average %HM DS  |         |     | 20 | 45 | 2   | 9  | 2  | 5   | 18   | 77   | 23 |

b)

|                       | Samples | Gr | St | Ky | Tur | Ep | Qz | Cal | ΣHM% | ΣLM% |
|-----------------------|---------|----|----|----|-----|----|----|-----|------|------|
|                       |         | rt | ta | ni | ma  | pi | ua | ci  |      |      |
| PLAGE MILITAIRE BEACH | Pms6a   | 9  | 25 | 5  | 15  | 5  | 6  | 34  | 60   | 40   |
|                       | Pms1a   | 28 | 38 | 3  | 19  | 4  | 3  | 5   | 92   | 8    |
|                       | Pms2a   | 32 | 46 | 1  | 11  | 2  | 1  | 8   | 91   | 9    |
|                       | Pms3a   | 38 | 50 | 2  | 2   | 1  | 1  | 5   | 94   | 6    |
|                       | Pms4a   | 39 | 45 | 2  | 6   | 1  | 2  | 4   | 94   | 6    |
|                       | Pms5a   | 36 | 41 | 2  | 16  | 0  | 2  | 3   | 95   | 5    |
|                       | Pms1b   | 9  | 44 | 1  | 24  | 4  | 1  | 15  | 83   | 17   |
|                       | Pms2b   | 37 | 41 | 2  | 15  | 1  | 0  | 3   | 96   | 4    |
|                       | Pms3b   | 29 | 50 | 1  | 15  | 1  | 2  | 3   | 95   | 5    |
|                       | Pms4b   | 14 | 53 | 2  | 16  | 1  | 1  | 13  | 86   | 14   |
|                       | Pms5b   | 35 | 48 | 0  | 10  | 0  | 4  | 4   | 92   | 8    |
|                       | Pms6b   | 19 | 46 | 0  | 21  | 2  | 1  | 12  | 88   | 13   |
|                       | Pms1C   | 32 | 55 | 1  | 7   | 1  | 0  | 3   | 97   | 3    |
|                       | Pms2c   | 35 | 41 | 1  | 17  | 0  | 1  | 5   | 94   | 6    |
|                       | Pms3c   | 33 | 52 | 4  | 6   | 0  | 1  | 3   | 95   | 5    |
|                       | Pms5c   | 29 | 52 | 2  | 11  | 0  | 1  | 5   | 93   | 7    |
|                       | Pms6c   | 46 | 39 | 1  | 10  | 2  | 0  | 2   | 98   | 2    |
| Average %HM DS        |         | 31 | 46 | 2  | 13  | 1  | 1  | 6   | 93   | 7    |

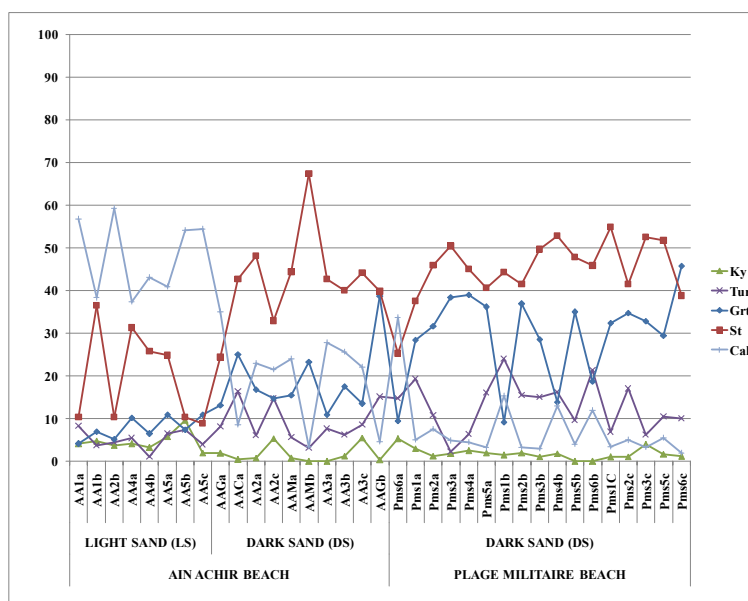


Figure.2. Percentage of the heavy and light minerals at Ain Achir sand beach and the Plage-Militaire. Ep: epidote, Grt: garnet, Ky: kyanite, St: staurolite, Tur: tourmaline, Qz: Quartz, Cal: calcite [9].

Rothwell, (1989) [10] has shown that the classification of heavy minerals can be based on the degree of transparency and on their resistance to weathering into two groups: ultrastable minerals (tourmaline) and metastable minerals (e.g. garnet, epidote, staurolite...). Analyses of the Ain Achir and Plage-Militaire dark sand have yielded a variegated spectrum of minerals (Fig.3) with dominantly metastable minerals: garnet, staurolite, epidote and kyanite and ultrastable heavy minerals e.g. tourmaline.

#### 4.1.1. Metastable minerals group

Staurolite: the mineral is well represented and it is the most common mineral in the two beaches. The crystals have dark yellowish brown colour. It occurs as irregular, elongated or fractured grains. Some crystals show inclusions.

Garnet: the grain occurs as euhedral, subrounded to rounded crystals. Some grains are sharp irregular fragments. Most of the crystals are pale-pink to orange-pale and some are pinkish brown. Ilmenite, apatite and quartz inclusions are common.

Epidote: Under the stereo-microscope epidote is pale green and elongated. Some grains have sub-rounded sharp.

Kyanite: this mineral is present in prismatic fragments. All crystals are sharp-edged, bluish-grey to pale blue varieties are common. Some crystals show small typical kyanite cleavage and exhibit characteristic step-like fractures, Ilmenite inclusions are common.

4.1.2. Ultrastable minerals group

Tourmaline: this mineral is fairly present; the grains are black irregular fragments with sharp edges or various degrees of rounding.

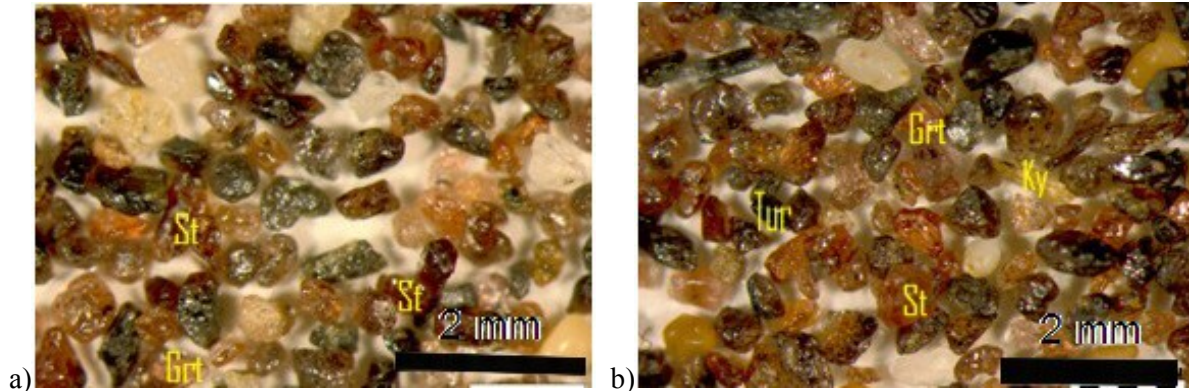


Figure.3. Photomicrograph under binocular microscope of the dark sand of : a) Ain Achir beach, b) Plage-Militaire beach. Ep: epidote, Grt: garnet, Ky: kyanite, St: staurolite, Tur: tourmaline, [9]

4.2. Sand chemistry

Majors, Traces element and REEs content of the Ain Achir beach and the Plage-Militaire sands and of the Upper Continental Crust (UCC) [11, 12, 13, 14] are shown in table 2.

Table 2. Abundance of major, trace and rare earth elements of: a) Ain Achir sand; b) Plage-Militaire. UCC: Upper Continental Crust, AV LS: average in light sand; AV DS: average in dark sand.

a)

|         | AIN ACHIR BEACH |       |       |       |       |       |       |       |       |        |                |       |       |       |       |       |       |       |       |        | UCC  |
|---------|-----------------|-------|-------|-------|-------|-------|-------|-------|-------|--------|----------------|-------|-------|-------|-------|-------|-------|-------|-------|--------|------|
|         | LIGHT SAND (LS) |       |       |       |       |       |       |       |       |        | DARK SAND (DS) |       |       |       |       |       |       |       |       |        |      |
|         | AA1a            | AA1b  | AA2b  | AA4a  | AA4b  | AA5a  | AA5b  | AA5c  | AA6a  | AV LS  | AACa           | AA2a  | AA2c  | AAMa  | AAMb  | AA3a  | AA3b  | AA3c  | AAGb  | AV DS  |      |
| SiO2    | 60.5            | 57.72 | 59.65 | 54.15 | 55.64 | 53.86 | 56.19 | 54.51 | 50.65 | 55.87  | 50.08          | 59.97 | 58.36 | 52.15 | 35.88 | 49.42 | 48.32 | 46.1  | 36.77 | 48.56  | 66.6 |
| TiO2    | 0.163           | 0.234 | 0.122 | 0.288 | 0.239 | 0.272 | 0.211 | 0.269 | 0.361 | 0.24   | 0.377          | 0.125 | 0.168 | 0.304 | 0.977 | 0.42  | 0.478 | 0.497 | 1.077 | 0.49   | 0.64 |
| Al2O3   | 5.44            | 7.53  | 4.11  | 8.99  | 7.42  | 8.38  | 6.77  | 8.53  | 10.45 | 7.51   | 12.66          | 3.85  | 5.62  | 10.48 | 27.72 | 13.48 | 14.73 | 16.4  | 24.38 | 14.37  | 15.4 |
| Fe2O3   | 3.1             | 4.81  | 1.62  | 5.62  | 5.25  | 4.55  | 3.83  | 5.05  | 7.52  | 4.59   | 8.77           | 1.86  | 3.02  | 6.57  | 28.73 | 11.44 | 11.38 | 13.2  | 26.29 | 12.36  | 5.04 |
| MnO     | 0.039           | 0.058 | 0.026 | 0.068 | 0.062 | 0.06  | 0.05  | 0.062 | 0.087 | 0.06   | 0.103          | 0.028 | 0.044 | 0.083 | 0.286 | 0.119 | 0.128 | 0.138 | 0.263 | 0.13   | 0.1  |
| MgO     | 1               | 1.12  | 1.04  | 1.3   | 1.23  | 1.37  | 1.23  | 1.29  | 1.46  | 1.23   | 1.35           | 1.03  | 1.16  | 1.39  | 1.92  | 1.27  | 1.42  | 1.44  | 1.86  | 1.43   | 2.48 |
| CaO     | 15.23           | 14.58 | 17.13 | 15.15 | 15.43 | 16.19 | 16.3  | 15.92 | 15.06 | 15.67  | 13.7           | 16.94 | 16.16 | 14.7  | 3.44  | 12.04 | 12.11 | 11.44 | 5.07  | 11.73  | 3.59 |
| Na2O    | 0.07            | 0.05  | 0.07  | 0.14  | 0.14  | 0.21  | 0.07  | 0.05  | 0.2   | 0.11   | 0.1            | 0.14  | 0.02  | 0.26  | 0.01  | 0.06  | 0.05  | 0.01  | 0.05  | 0.08   | 3.27 |
| K2O     | 0.51            | 0.48  | 0.55  | 0.46  | 0.53  | 0.49  | 0.5   | 0.47  | 0.37  | 0.48   | 0.28           | 0.63  | 0.38  | 0.4   | 0.07  | 0.33  | 0.34  | 0.25  | 0.11  | 0.31   | 2.8  |
| P2O5    | 0.048           | 0.059 | 0.044 | 0.071 | 0.058 | 0.078 | 0.06  | 0.071 | 0.084 | 0.06   | 0.072          | 0.044 | 0.054 | 0.07  | 0.13  | 0.078 | 0.082 | 0.09  | 0.134 | 0.08   | 0.15 |
| LOI     | 13.69           | 13.16 | 15.47 | 13.5  | 13.72 | 14.21 | 14.58 | 13.6  | 13.46 | 13.93  | 12.21          | 15.13 | 14.86 | 13.22 | 0.53  | 11.04 | 10.67 | 10.27 | 3.73  | 10.18  |      |
| Ba      | 57              | 70    | 66    | 43    | 64    | 52    | 53    | 50    | 61    | 57.33  | 60             | 62    | 56    | 60    | 36    | 45    | 49    | 51    | 79    | 55.33  | 628  |
| Cr      | 22              | 33    | 15    | 38    | 32    | 32    | 28    | 34    | 58    | 32.44  | 68             | 13    | 25    | 56    | 132   | 58    | 68    | 76    | 132   | 69.78  | 92   |
| Ga      | 10              | 11    | 10    | 14    | 11    | 12    | 10    | 14    | 17    | 12.11  | 21             | 10    | 10    | 18    | 43    | 19    | 23    | 24    | 34    | 22.44  | 17.5 |
| Nb      | 10              | 10    | 10    | 10    | 10    | 10    | 10    | 10    | 10    | 10.00  | 10             | 10    | 10    | 10    | 15    | 10    | 10    | 10    | 18    | 11.44  | 12   |
| Ni      | 13              | 10    | 10    | 10    | 10    | 17    | 10    | 13    | 10    | 11.44  | 10             | 10    | 10    | 10    | 21    | 12    | 14    | 20    | 11    | 13.11  | 47   |
| Sr      | 458             | 413   | 487   | 451   | 460   | 494   | 477   | 461   | 579   | 475.56 | 477            | 489   | 449   | 564   | 57    | 313   | 333   | 332   | 145   | 351.00 | 320  |
| V       | 23              | 26    | 22    | 38    | 33    | 36    | 26    | 37    | 37    | 30.89  | 45             | 16    | 21    | 48    | 101   | 59    | 56    | 58    | 86    | 54.44  | 97   |
| Y       | 19              | 23    | 12    | 24    | 25    | 22    | 20    | 24    | 36    | 22.78  | 44             | 12    | 17    | 34    | 107   | 46    | 49    | 57    | 120   | 54.00  | 21   |
| Zn      | 68              | 94    | 39    | 121   | 91    | 114   | 86    | 116   | 142   | 96.78  | 177            | 35    | 80    | 151   | 394   | 178   | 216   | 236   | 349   | 201.78 | 67   |
| Zr      | 64              | 77    | 47    | 86    | 71    | 84    | 69    | 86    | 151   | 81.67  | 157            | 47    | 55    | 133   | 240   | 119   | 129   | 153   | 325   | 150.89 | 193  |
| La      | 10.21           | 12.4  | 8.8   | 21.9  | 13.2  | 15.2  | 12.9  | 15.1  | 41.1  | 16.74  | 21.2           | 8.5   | 10.7  | 17.0  | 44.0  | 27.2  | 23.1  | 23.8  | 18.1  | 21.51  | 31   |
| Ce      | 20.379          | 27.2  | 17.0  | 31.2  | 26.7  | 29.5  | 24.6  | 29.1  | 83.9  | 32.17  | 40.0           | 16.2  | 21.2  | 33.5  | 89.5  | 45.8  | 48.6  | 55.4  | 34.5  | 42.74  | 63   |
| Pr      | 1.9409          | 2.6   | 1.6   | 3.0   | 2.7   | 2.7   | 2.6   | 2.8   | 9.1   | 3.22   | 4.1            | 1.6   | 1.9   | 3.3   | 9.8   | 4.6   | 5.2   | 5.3   | 3.1   | 4.33   | 7.1  |
| Nd      | 9.603           | 12.3  | 8.3   | 14.2  | 12.5  | 14.3  | 11.9  | 13.7  | 36.4  | 14.81  | 17.9           | 8.1   | 9.9   | 15.3  | 38.6  | 20.1  | 21.6  | 23.4  | 15.5  | 18.92  | 27   |
| Sm      | 1.902           | 2.4   | 1.7   | 2.9   | 2.5   | 2.9   | 2.5   | 3.0   | 7.6   | 3.03   | 3.7            | 1.6   | 2.0   | 3.2   | 8.1   | 4.1   | 4.4   | 4.8   | 3.3   | 3.90   | 4.7  |
| Eu      | 0.447           | 0.5   | 0.4   | 0.6   | 0.5   | 0.6   | 0.5   | 0.6   | 1.1   | 0.57   | 0.6            | 0.4   | 0.4   | 0.6   | 1.2   | 0.7   | 0.7   | 0.8   | 0.6   | 0.69   | 1    |
| Gd      | 2.085           | 2.7   | 1.7   | 3.1   | 2.9   | 3.0   | 2.6   | 3.1   | 9.2   | 3.38   | 4.1            | 1.7   | 2.1   | 3.4   | 10.1  | 4.8   | 5.1   | 5.5   | 3.6   | 4.48   | 4    |
| Tb      | 0.378           | 0.5   | 0.3   | 0.6   | 0.5   | 0.6   | 0.5   | 0.9   | 2.1   | 0.73   | 0.9            | 0.3   | 0.4   | 0.8   | 2.3   | 1.0   | 1.1   | 1.2   | 0.8   | 0.97   | 0.7  |
| Dy      | 2.49            | 3.6   | 1.6   | 4.0   | 3.9   | 3.4   | 3.0   | 3.8   | 15.1  | 4.54   | 5.6            | 1.7   | 2.4   | 4.3   | 17.3  | 7.6   | 7.6   | 8.4   | 4.7   | 6.62   | 3.9  |
| Ho      | 0.532           | 0.8   | 0.3   | 0.8   | 0.9   | 0.7   | 0.6   | 0.8   | 3.4   | 0.99   | 1.2            | 0.4   | 0.5   | 0.9   | 4.0   | 1.7   | 1.7   | 1.9   | 1.0   | 1.48   | 0.83 |
| Er      | 1.618           | 2.4   | 0.9   | 2.6   | 2.5   | 2.2   | 1.9   | 2.4   | 10.6  | 3.02   | 3.9            | 1.0   | 1.5   | 2.9   | 12.5  | 5.3   | 5.2   | 5.9   | 3.3   | 4.61   | 2.3  |
| Tm      | 0.255           | 0.4   | 0.2   | 0.4   | 0.5   | 0.3   | 0.3   | 0.3   | 1.6   | 0.48   | 0.6            | 0.2   | 0.3   | 0.5   | 2.0   | 0.9   | 0.8   | 1.0   | 0.5   | 0.75   | 0.3  |
| Yb      | 1.6             | 2.4   | 0.9   | 2.5   | 2.5   | 2.1   | 1.8   | 2.4   | 10.3  | 2.94   | 3.9            | 1.0   | 1.5   | 2.8   | 12.1  | 5.2   | 5.1   | 5.8   | 3.1   | 4.52   | 2    |
| Lu      | 0.23            | 0.3   | 0.1   | 0.4   | 0.4   | 0.3   | 0.3   | 0.3   | 1.5   | 0.42   | 0.6            | 0.2   | 0.2   | 0.5   | 1.7   | 0.7   | 0.7   | 0.8   | 0.5   | 0.66   | 0.31 |
| ΣTraces | 744             | 767   | 718   | 835   | 807   | 873   | 789   | 845   | 1101  | 831.00 | 1069           | 704   | 733   | 1084  | 1146  | 859   | 947   | 1017  | 1299  | 984    | 1495 |
| ΣLREE   | 44              | 57    | 37    | 73    | 58    | 65    | 54    | 64    | 178   | 70     | 87             | 36    | 46    | 72    | 190   | 102   | 103   | 113   | 74    | 91     | 133  |
| ΣHREE   | 10              | 14    | 6     | 15    | 15    | 13    | 12    | 14    | 55    | 17     | 21             | 7     | 9     | 17    | 63    | 28    | 28    | 31    | 18    | 25     | 15   |
| ΣREE    | 54              | 71    | 44    | 88    | 72    | 78    | 66    | 78    | 233   | 87     | 108            | 43    | 55    | 89    | 253   | 130   | 131   | 144   | 93    | 116    | 148  |

b)

| PLAGE MILITAIRE BEACH          |       |       |       |       |       |       |       |       |       |       |       |       |       |       |       |       |       |        |      |
|--------------------------------|-------|-------|-------|-------|-------|-------|-------|-------|-------|-------|-------|-------|-------|-------|-------|-------|-------|--------|------|
| DARK SAND                      |       |       |       |       |       |       |       |       |       |       |       |       |       |       |       |       |       |        |      |
|                                | Pms6a | Pms1a | Pms2a | Pms3a | Pms4a | Pms5a | Pms1b | Pms2b | Pms3b | Pms4b | Pms5b | Pms6b | Pms1C | Pms2c | Pms3c | Pms5c | Pms6c | AV     | UCC  |
| SiO <sub>2</sub>               | 34,3  | 33,4  | 34,3  | 32,62 | 36,54 | 47,08 | 41,53 | 34,95 | 34,5  | 40,68 | 38,87 | 37,31 | 34,62 | 33,71 | 34,69 | 35,41 | 35,31 | 36,5   | 66,6 |
| TiO <sub>2</sub>               | 0,887 | 0,792 | 0,878 | 0,84  | 0,796 | 0,457 | 0,715 | 0,841 | 0,871 | 0,673 | 0,758 | 0,806 | 0,881 | 0,795 | 0,872 | 0,879 | 0,91  | 0,8    | 0,64 |
| Al <sub>2</sub> O <sub>3</sub> | 28,85 | 25,77 | 28,41 | 24,71 | 25,42 | 15,27 | 23,39 | 26,88 | 28,11 | 22,33 | 24,02 | 25,05 | 28,6  | 25,44 | 27,83 | 26,53 | 26,27 | 25,5   | 15,4 |
| Fe <sub>2</sub> O <sub>3</sub> | 26,83 | 30,73 | 30,2  | 34,81 | 26,13 | 11,4  | 19,16 | 27,63 | 29,26 | 19,23 | 21,96 | 22,94 | 28,18 | 30,01 | 29,69 | 27,65 | 27,5  | 26,1   | 5,04 |
| MnO                            | 0,29  | 0,281 | 0,324 | 0,295 | 0,282 | 0,135 | 0,21  | 0,278 | 0,314 | 0,225 | 0,24  | 0,248 | 0,301 | 0,271 | 0,317 | 0,29  | 0,285 | 0,3    | 0,1  |
| MgO                            | 1,77  | 1,68  | 1,87  | 1,76  | 1,69  | 1,3   | 1,62  | 1,71  | 1,86  | 1,51  | 1,64  | 1,68  | 1,82  | 1,68  | 1,86  | 1,81  | 1,84  | 1,7    | 2,48 |
| CaO                            | 3,73  | 4,01  | 2,4   | 2,91  | 4,99  | 12,65 | 10,48 | 4,22  | 2,83  | 8,08  | 6,74  | 6,48  | 3,13  | 4,47  | 2,74  | 4,22  | 4,34  | 5,2    | 3,59 |
| Na <sub>2</sub> O              | 0,05  | 0,1   | 0,01  | 0,01  | 0,03  | 0,1   | 0,01  | 0,01  | 0,01  | 0,01  | 0,08  | 0,01  | 0,04  | 0,01  | 0,01  | 0,01  | 0,01  | 0,0    | 3,27 |
| K <sub>2</sub> O               | 0,07  | 0,07  | 0,05  | 0,05  | 0,1   | 0,3   | 0,17  | 0,08  | 0,05  | 0,17  | 0,13  | 0,11  | 0,06  | 0,08  | 0,06  | 0,08  | 0,08  | 0,1    | 2,8  |
| P <sub>2</sub> O <sub>5</sub>  | 0,104 | 0,099 | 0,111 | 0,103 | 0,1   | 0,063 | 0,091 | 0,103 | 0,111 | 0,083 | 0,094 | 0,093 | 0,106 | 0,097 | 0,108 | 0,107 | 0,107 | 0,1    | 0,15 |
| LOI                            | 11,3  | 2,85  | 2,96  | 1,26  | 1,61  | 3,72  | 2,43  | 3,16  | 1,84  | 6,79  | 5,21  | 5,05  | 1,98  | 3,28  | 1,64  | 2,88  | 3,13  | 3,6    |      |
| Ba                             | 51    | 42    | 32    | 13    | 30    | 44    | 39    | 34    | 50    | 34    | 52    | 22    | 33    | 40    | 33    | 23    | 46    | 36,4   | 628  |
| Cr                             | 125   | 113   | 125   | 111   | 112   | 67    | 104   | 116   | 123   | 95    | 104   | 109   | 122   | 112   | 121   | 114   | 55    | 107,5  | 92   |
| Ga                             | 44    | 39    | 44    | 36    | 38    | 22    | 35    | 43    | 39    | 33    | 38    | 38    | 42    | 42    | 39    | 36    | 117   | 42,6   | 17,5 |
| Nb                             | 12    | 11    | 10    | 10    | 9     | 9     | 10    | 10    | 9     | 10    | 10    | 11    | 9     | 10    | 9     | 10    | 38    | 11,6   | 12   |
| Ni                             | 16    | 15    | 17    | 18    | 17    | 12    | 15    | 18    | 19    | 16    | 18    | 14    | 17    | 15    | 22    | 13    | 13    | 16,2   | 47   |
| Sr                             | 60    | 71    | 19    | 41    | 92    | 307   | 235   | 78    | 30    | 174   | 145   | 133   | 41    | 85    | 28    | 69    | 24    | 96,0   | 320  |
| V                              | 96    | 91    | 97    | 86    | 88    | 53    | 77    | 94    | 95    | 76    | 79    | 93    | 98    | 88    | 94    | 96    | 74    | 86,8   | 97   |
| Y                              | 110   | 117   | 135   | 134   | 115   | 53    | 75    | 113   | 128   | 90    | 96    | 96    | 119   | 116   | 129   | 119   | 101   | 108,6  | 21   |
| Zn                             | 437   | 410   | 410   | 367   | 377   | 234   | 359   | 418   | 402   | 331   | 358   | 379   | 435   | 399   | 397   | 377   | 115   | 365,0  | 67   |
| Zr                             | 235   | 226   | 230   | 229   | 209   | 132   | 196   | 227   | 232   | 183   | 199   | 201   | 232   | 228   | 225   | 217   | 382   | 222,5  | 193  |
| La                             | 42,0  | 41,1  | 42,9  | 46,0  | 40,9  | 24,1  | 33,0  | 40,3  | 44,3  | 34,6  | 36,3  | 36,8  | 41,7  | 42,4  | 42,2  | 41,0  | 41,1  | 39,4   | 31   |
| Ce                             | 84,0  | 84,1  | 87,2  | 93,3  | 82,6  | 47,4  | 65,8  | 80,9  | 90,1  | 69,7  | 72,1  | 74,4  | 84,4  | 85,5  | 85,1  | 83,4  | 82,3  | 79,6   | 63   |
| Pr                             | 9,2   | 9,1   | 9,6   | 10,2  | 8,9   | 5,1   | 7,2   | 8,8   | 9,9   | 7,5   | 8,0   | 8,0   | 9,2   | 9,4   | 9,1   | 9,1   | 9,1   | 8,7    | 7,1  |
| Nd                             | 36,5  | 36,5  | 37,8  | 40,3  | 36,0  | 21,2  | 29,1  | 35,3  | 39,4  | 30,6  | 31,6  | 32,8  | 36,5  | 37,4  | 37,0  | 36,1  | 36,1  | 34,7   | 27   |
| Sm                             | 7,6   | 7,7   | 8,1   | 8,5   | 7,6   | 4,3   | 6,0   | 7,4   | 8,4   | 6,4   | 6,6   | 6,8   | 7,7   | 7,9   | 7,8   | 7,7   | 7,6   | 7,3    | 4,7  |
| Eu                             | 1,2   | 1,2   | 1,3   | 1,3   | 1,2   | 0,7   | 0,9   | 1,2   | 1,3   | 1,0   | 1,0   | 1,1   | 1,2   | 1,2   | 1,3   | 1,2   | 1,2   | 1,1    | 1    |
| Gd                             | 9,5   | 9,8   | 10,9  | 11,1  | 9,7   | 4,9   | 6,9   | 9,5   | 11,0  | 7,8   | 8,2   | 8,6   | 9,9   | 9,8   | 10,4  | 9,9   | 9,8   | 9,3    | 4    |
| Tb                             | 2,0   | 2,2   | 2,6   | 2,6   | 2,3   | 1,0   | 1,5   | 2,1   | 2,6   | 1,8   | 1,8   | 2,0   | 2,2   | 2,3   | 2,4   | 2,3   | 2,2   | 2,1    | 0,7  |
| Dy                             | 16,4  | 17,9  | 21,0  | 21,1  | 18,2  | 7,5   | 11,2  | 16,9  | 21,0  | 13,9  | 14,2  | 15,5  | 17,7  | 17,8  | 19,5  | 18,4  | 17,7  | 16,8   | 3,9  |
| Ho                             | 3,7   | 4,1   | 4,9   | 4,9   | 4,2   | 1,7   | 2,6   | 3,9   | 4,9   | 3,2   | 3,3   | 3,6   | 4,1   | 4,1   | 4,5   | 4,3   | 4,0   | 3,9    | 0,83 |
| Er                             | 11,8  | 13,2  | 15,4  | 15,4  | 13,4  | 5,4   | 8,0   | 12,2  | 15,5  | 10,3  | 10,3  | 11,3  | 13,0  | 12,9  | 14,2  | 13,5  | 12,7  | 12,2   | 2,3  |
| Tm                             | 1,9   | 2,0   | 2,4   | 2,3   | 2,0   | 0,8   | 1,2   | 1,9   | 2,4   | 1,6   | 1,6   | 1,7   | 2,0   | 2,0   | 2,2   | 2,1   | 2,0   | 1,9    | 0,3  |
| Yb                             | 11,6  | 12,8  | 15,0  | 14,6  | 13,0  | 5,3   | 7,8   | 12,0  | 14,9  | 9,9   | 10,0  | 10,9  | 12,7  | 12,4  | 13,9  | 12,9  | 12,3  | 11,9   | 2    |
| Lu                             | 1,6   | 1,8   | 2,1   | 2,0   | 1,8   | 0,7   | 1,1   | 1,7   | 2,1   | 1,4   | 1,4   | 1,5   | 1,8   | 1,7   | 2,0   | 1,8   | 1,7   | 1,7    | 0,31 |
| ΣTraces                        | 1186  | 1135  | 1119  | 1045  | 1087  | 933   | 1145  | 1151  | 1127  | 1042  | 1099  | 1096  | 1148  | 1135  | 1097  | 1074  | 965   | 1093,2 | 1495 |
| ΣLREE                          | 179   | 178   | 186   | 198   | 176   | 102   | 141   | 173   | 192   | 149   | 154   | 159   | 179   | 183   | 181   | 177   | 176   | 169,7  | 133  |
| ΣHREE                          | 60    | 65    | 75    | 75    | 66    | 28    | 41    | 61    | 76    | 51    | 52    | 56    | 65    | 64    | 70    | 66    | 64    | 60,9   | 15   |
| ΣREE                           | 239   | 244   | 261   | 274   | 242   | 130   | 182   | 234   | 268   | 200   | 206   | 215   | 244   | 247   | 252   | 243   | 240   | 230,6  | 148  |

At Ain Achir beach, the light sand and the dark one show some differences in the chemical compositions. At Ain Achir the average concentrations of some Major elements (TiO<sub>2</sub>=0.24, Al<sub>2</sub>O<sub>3</sub>=7.51, Fe<sub>2</sub>O<sub>3</sub>=4.59, MnO=0.6, MgO=1.23 and P<sub>2</sub>O<sub>5</sub>=0.06 wt %) are lower than in the dark one (TiO<sub>2</sub>=0.49, Al<sub>2</sub>O<sub>3</sub>=14.37, Fe<sub>2</sub>O<sub>3</sub>=12.36, MnO=0.13, MgO=1.43 and P<sub>2</sub>O<sub>5</sub>=0.08wt%). Whereas CaO=15.67, Na<sub>2</sub>O=0.11, K<sub>2</sub>O=0.48 wt% are higher (CaO=11.73, Na<sub>2</sub>O=0.08, K<sub>2</sub>O=0.31wt%). The dark sand of Plage-Militaire beach is enriched in TiO<sub>2</sub>=0.8wt%, Al<sub>2</sub>O<sub>3</sub>=26.27wt%, Fe<sub>2</sub>O<sub>3</sub>=26.1wt%, MnO=0.3wt%, MgO=1.7wt% and P<sub>2</sub>O<sub>5</sub>=0.1wt%. Compared to the UCC composition (Tab.2), the dark sand of Ain Achir and Plage-Militaire beaches show higher Majors concentration values.

The total of trace elements (Ba, Cr, Ga, Nb, Ni, V, Y, Zn and Zr) in the Ain Achir light sand and in the dark one is respectively 831ppm and 984ppm. These concentrations are lower than the UCC traces element concentration (1495ppm). The Plage-Militaire beach is also characterized by very high concentration in trace elements (total 1093ppm), this value is higher than at Ain Achir beach and is more close to the UCC total traces element concentration (Tab.2), (Fig.4a).

The REE concentrations vary widely for the two beaches (ΣREE=87-230ppm) and are low in the Ain Achir sands (Tab.2), (Fig.4b). At Ain Achir beach the REE abundances (ΣREE=87-116ppm) is less than that of the ΣREE Upper Continental Crust (ΣREE<sub>UCC</sub>=148ppm), [12, 13, 14], whereas the REE abundance at Plage-Militaire beach is slightly higher (ΣREE=230ppm). The ΣREE content at Ain Achir beach is 87ppm and 116ppm, respectively for the light and dark sand. Ain Achir sands show that they are mainly high in LREE (ΣLREE=70-91ppm) rather than HREE (ΣHREE=17-15ppm). The dark sand show higher LREE and HREE concentration (ΣLREE=91ppm and ΣHREE=25ppm) than the light sand. In regard to the UCC (ΣHREE<sub>UCC</sub>=15ppm), the total of HREE (ΣHREE= 25ppm) of the dark sand is also high. Compared to the Ain Achir sand and to the ΣREE of the Upper Continental Crust (ΣREE<sub>UCC</sub>=148ppm) [12, 13, 14], the ΣREE concentration of the Plage-Militaire black sand is remarkably high (ΣREE=230ppm).

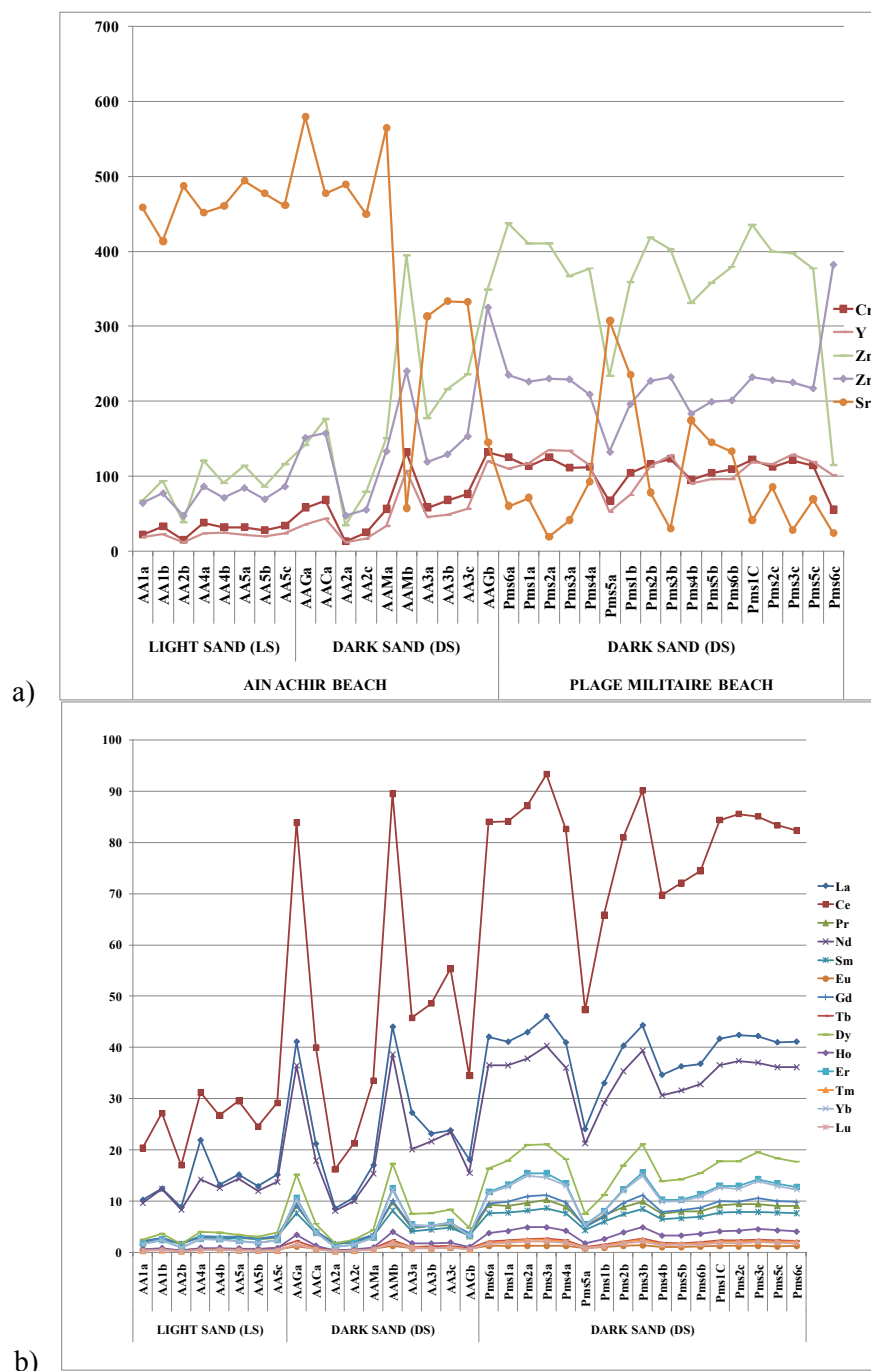


Figure.4. a) Distribution of trace elements in the Ain Achir and Plage-Mititaire sand; b) Distribution of Rare Earth Elements in the Ain Achir and Plage-Militaire sands.

## 5. DISCUSSION

### 5.1. Simple statistical analysis

Major elements: compared to the dark sand of Ain Achir and the Plage-Militaire (Fig.5) the Ain Achir light sand is rich in CaO, Na<sub>2</sub>O and K<sub>2</sub>O. Enrichments in CaO are due to the occurrence of high modal concentration of carbonate minerals in this sand, whereas the high values in K<sub>2</sub>O and Na<sub>2</sub>O reflect the presence of clays minerals. The high P<sub>2</sub>O<sub>5</sub> concentration in the dark sand of the two beaches corresponds to apatite inclusions in some garnet and staurolite grain. The figure 5 shows also that those dark sands are enriched in Fe<sub>2</sub>O<sub>3</sub>, MgO and TiO<sub>2</sub>, these high values are in accordance with the modal high heavy-mineral (i.e. garnet, staurolite) and their inclusions (i.e. ilmenite) contents. The selected major elements content increases with increasing the modal content in heavy minerals.

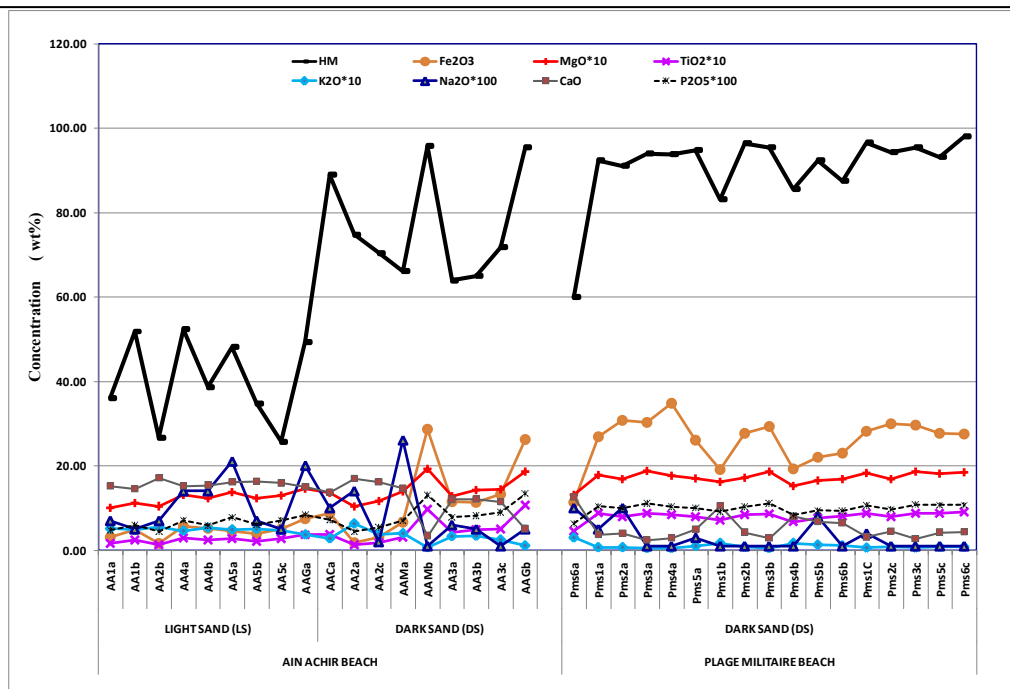


Figure.5. Heavy minerals (HM) and Major elements variations in the Ain Achir and Plage-Militaire Sands.

*Traces and REE elements:* in order to explore the possible relationship existing between the different chemical elements (traces and REEs) and the mineralogical composition of Ain Achir and Plage-Militaire sand, simple statistical methods such as correlation and factor analysis have been used. Correlation and factor analysis have been performed for traces and rare earth elements using the software XLSTAT-PRO 7.5. Table 3 shows correlation matrix for the trace, REE and heavy mineral amount.

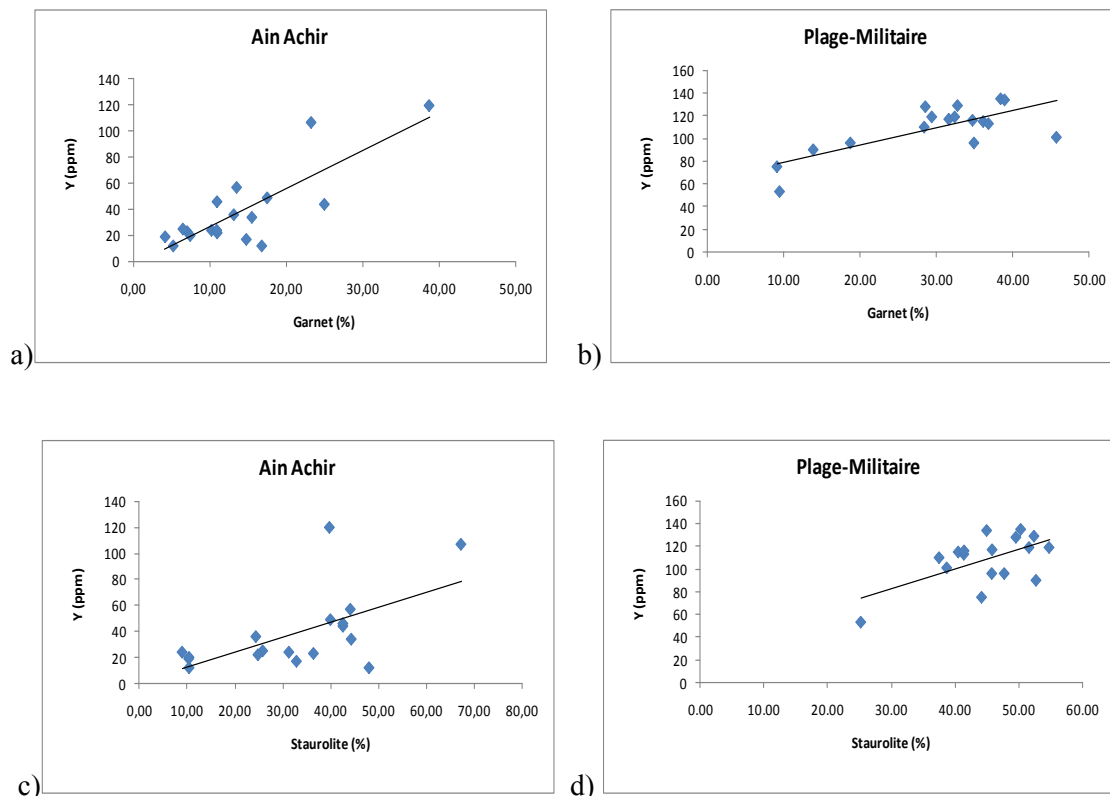
Table 3. Correlation coefficients (r) between the mineralogical and trace elements composition, a) Ain Achir sand, b) Plage-Militaire sand. Ep: epidote, Grt: garnet, Ky: kyanite, St: staurolite, Tur: tourmaline, Qz: quartz, Cal: Cacite, [9]

| a) Variables |       |       |       |       |       |       |       | b) Variables |       |       |        |       |       |       |       |
|--------------|-------|-------|-------|-------|-------|-------|-------|--------------|-------|-------|--------|-------|-------|-------|-------|
|              | Grt   | St    | Ky    | Tur   | Ep    | Qz    | Cal   |              | Grt   | St    | Ky     | Tur   | Ep    | Qz    | Cal   |
| Grt          | 1     |       |       |       |       |       |       | Grt          | 1     |       |        |       |       |       |       |
| St           | 0.60  | 1.00  |       |       |       |       |       | St           | 0.18  | 1.00  |        |       |       |       |       |
| Ky           | -0.56 | -0.56 | 1.00  |       |       |       |       | Ky           | -0.25 | -0.49 | 1.00   |       |       |       |       |
| Tur          | 0.59  | 0.11  | -0.07 | 1.00  |       |       |       | Tur          | -0.62 | -0.38 | -0.11  | 1.00  |       |       |       |
| Ep           | -0.10 | -0.16 | -0.16 | 0.27  | 1.00  |       |       | Ep           | -0.58 | -0.64 | 0.44   | 0.41  | 1.00  |       |       |
| Qz           | -0.69 | -0.70 | 0.31  | -0.53 | -0.26 | 1.00  | 0.76  | Qz           | -0.44 | -0.59 | 0.58   | 0.09  | 0.47  | 1.00  |       |
| Cal          | -0.85 | -0.90 | 0.57  | -0.48 | 0.10  | 0.76  | 1.00  | Cal          | -0.82 | -0.57 | 0.50   | 0.36  | 0.69  | 0.70  | 1.00  |
| Ba           | 0.23  | -0.23 | 0.04  | 0.32  | 0.04  | -0.15 | 0.06  | Ba           | -0.06 | -0.31 | 0.00   | 0.20  | 0.34  | 0.33  | 0.08  |
| Cr           | 0.68  | 0.54  | -0.45 | 0.18  | 0.06  | -0.57 | -0.61 | Cr           | 0.17  | 0.57  | -0.18  | -0.11 | -0.42 | -0.32 | -0.50 |
| Ga           | 0.62  | 0.59  | -0.45 | 0.09  | 0.07  | -0.58 | -0.61 | Ga           | 0.55  | -0.10 | -0.25  | -0.17 | 0.01  | -0.44 | -0.40 |
| Nb           | 0.79  | 0.40  | -0.37 | 0.26  | -0.03 | -0.56 | -0.57 | Nb           | 0.39  | -0.23 | -0.16  | -0.09 | 0.16  | -0.28 | -0.20 |
| Ni           | 0.19  | 0.46  | 0.13  | -0.06 | -0.25 | -0.40 | -0.36 | Ni           | 0.34  | 0.50  | 0.04   | -0.36 | -0.49 | -0.19 | -0.54 |
| Sr           | -0.64 | -0.63 | 0.39  | -0.11 | 0.04  | 0.64  | 0.64  | Sr           | -0.84 | -0.50 | 0.27   | 0.55  | 0.57  | 0.67  | 0.89  |
| V            | 0.64  | 0.61  | -0.45 | 0.11  | -0.02 | -0.57 | -0.64 | V            | 0.47  | 0.64  | -0.38  | -0.22 | -0.54 | -0.66 | -0.76 |
| Y            | 0.73  | 0.53  | -0.43 | 0.21  | 0.01  | -0.60 | -0.63 | Y            | 0.74  | 0.58  | -0.21  | -0.57 | -0.67 | -0.58 | -0.84 |
| Zn           | 0.66  | 0.58  | -0.42 | 0.16  | 0.02  | -0.58 | -0.64 | Zn           | 0.03  | 0.48  | -0.16  | 0.00  | -0.35 | -0.22 | -0.35 |
| Zr           | 0.72  | 0.42  | -0.43 | 0.27  | 0.08  | -0.54 | -0.57 | Zr           | 0.71  | 0.09  | -0.32  | -0.27 | -0.15 | -0.61 | -0.63 |
| La           | 0.22  | 0.40  | -0.38 | -0.12 | 0.08  | -0.14 | -0.35 | La           | 0.78  | 0.50  | -0.33  | -0.42 | -0.59 | -0.67 | -0.91 |
| Ce           | 0.26  | 0.44  | -0.34 | -0.08 | 0.03  | -0.20 | -0.39 | Ce           | 0.77  | 0.52  | -0.33  | -0.42 | -0.60 | -0.67 | -0.90 |
| Pr           | 0.23  | 0.42  | -0.35 | -0.11 | 0.03  | -0.17 | -0.36 | Pr           | 0.78  | 0.51  | -0.32  | -0.43 | -0.59 | -0.66 | -0.90 |
| Nd           | 0.25  | 0.42  | -0.34 | -0.08 | 0.02  | -0.19 | -0.38 | Nd           | 0.77  | 0.51  | -0.34  | -0.41 | -0.60 | -0.68 | -0.90 |
| Sm           | 0.27  | 0.42  | -0.35 | -0.06 | 0.04  | -0.20 | -0.39 | Sm           | 0.76  | 0.54  | -0.35  | -0.44 | -0.62 | -0.68 | -0.89 |
| Eu           | 0.29  | 0.45  | -0.31 | -0.06 | 0.00  | -0.23 | -0.41 | Eu           | 0.77  | 0.49  | -0.30  | -0.40 | -0.59 | -0.68 | -0.90 |
| Gd           | 0.26  | 0.44  | -0.35 | -0.08 | 0.02  | -0.20 | -0.39 | Gd           | 0.79  | 0.54  | -0.29  | -0.51 | -0.63 | -0.65 | -0.88 |
| Tb           | 0.31  | 0.45  | -0.39 | -0.02 | 0.06  | -0.24 | -0.43 | Tb           | 0.76  | 0.54  | -0.29  | -0.52 | -0.65 | -0.64 | -0.84 |
| Dy           | 0.26  | 0.46  | -0.36 | -0.10 | 0.02  | -0.21 | -0.40 | Dy           | 0.77  | 0.55  | -0.27  | -0.54 | -0.65 | -0.62 | -0.84 |
| Ho           | 0.25  | 0.47  | -0.36 | -0.11 | 0.02  | -0.21 | -0.40 | Ho           | 0.76  | 0.56  | -0.27  | -0.54 | -0.66 | -0.62 | -0.84 |
| Er           | 0.26  | 0.47  | -0.37 | -0.10 | 0.03  | -0.22 | -0.40 | Er           | 0.75  | 0.56  | -0.27  | -0.54 | -0.66 | -0.61 | -0.83 |
| Tm           | 0.25  | 0.48  | -0.35 | -0.11 | 0.01  | -0.22 | -0.40 | Tm           | 0.76  | 0.55  | -0.26  | -0.54 | -0.65 | -0.62 | -0.84 |
| Yb           | 0.25  | 0.47  | -0.37 | -0.11 | 0.03  | -0.22 | -0.40 | Yb           | 0.76  | 0.56  | -0.26  | -0.54 | -0.66 | -0.62 | -0.84 |
| Lu           | 0.28  | 0.48  | -0.39 | -0.09 | 0.02  | -0.23 | -0.42 | Lu           | 0.77  | 0.56  | -0.265 | -0.55 | -0.65 | -0.63 | -0.85 |



Trace elements correlation analysis of the two beaches shows that Cr, Ni, V, Y, Zn and Zr are positively correlated with garnet and staurolite. At Ain Achir, these elements show positive correlation with garnet ( $r_{Cr}=0.68$ ,  $r_{Ni}=0.19$ ,  $r_V=0.64$ ,  $r_Y=0.73$ ,  $r_{Zn}=0.66$ , and  $r_{Zr}=0.72$ ) and with staurolite ( $r_{Cr}=0.54$ ,  $r_{Ni}=0.46$ ,  $r_V=0.61$ ,  $r_Y=0.53$ ,  $r_{Zn}=0.58$  and  $r_{Zr}=0.42$ ). At the Plage-Militaire some of these elements are also positively correlated to garnet ( $r_{Ni}=0.34$ ,  $r_V=0.47$ ,  $r_Y=0.74$ , and  $r_{Zr}=0.71$ ) and to the staurolite ( $r_{Cr}=0.57$ ,  $r_{Ni}=0.5$ ,  $r_V=0.64$ ,  $r_Y=0.58$  and  $r_{Zn}=0.48$ ). At these beaches chromium and vanadium are significantly correlated to garnet and staurolite: Ain Achir (garnet  $r_{Cr}=0.68$ ,  $r_V=0.17$ ; staurolite  $r_{Cr}=0.51$ ,  $r_V=0.61$ ) and at the Plage-Militaire (garnet  $r_{Cr}=0.17$ ,  $r_V=0.47$ ; staurolite  $r_{Cr}=0.57$ ,  $r_V=0.64$ ) suggesting the presence of mafic minerals (i.e amphiboles, micas, epidote) inclusions in these minerals. The high positive correlation of yttrium with garnet of Ain Achir:  $r=0.73$  (Fig.6a), Plage-Militaire:  $r=0.74$  (Fig.6b) and staurolite: Ain Achir  $r=0.53$  (Fig.6c), Plage-Militaire  $r=0.58$  (Fig.6d) in the sand of the two beaches is related to more garnet and staurolite in these sand than the others heavy minerals. The significant correlation between Zn and the garnet of Ain Achir beach (Fig.6e) and the staurolite at the Plage-Militaire (Fig.6f) suggest the influence of the amount of each mineral. There is a strong interrelationship between Zr and garnet  $r=0.72$  at Ain Achir (Fig.6g) and  $r=0.71$  at Plage-Militaire (Fig.6h) confirming the presence of zircon inclusions in the garnet. In the two beaches, strontium is strongly correlated to calcite and quartz. The correlation with calcite ( $r=0.64$  at Ain Achir and  $r=0.89$  at Plage-Militaire) can be explained by the occurrence of some diagenetic calcite, whereas the positive correlation of Sr with quartz ( $r=0.64$  at Ain Achir and  $r=0.67$  at Plage-Militaire beach) reflects de nature of the quartz. Monecke, et al; 2002 [14], show that some trace element contents of hydrothermal and metamorphic quartz are higher than in magmatic one.

Table 3 shows that the REE of the Plage-Militaire sand are more correlated to garnet ( $r > 0.75$ ) than at the Ain Achir ( $r < 0.3$ ), REE are more linked to sands with high modal heavy mineral content (i.e. garnet and staurolite). This slight enrichment in REE of the dark sand of the Plage-Militaire can also be explained by its low concentration in carbonates and clay phases. The correlation between REE and the other heavy minerals (kyanite, tourmaline and epidote) for the two beaches is not statistically significant which confirm that REEs are mainly hosted in the heavy minerals (garnet and staurolite) rather than in the other one.



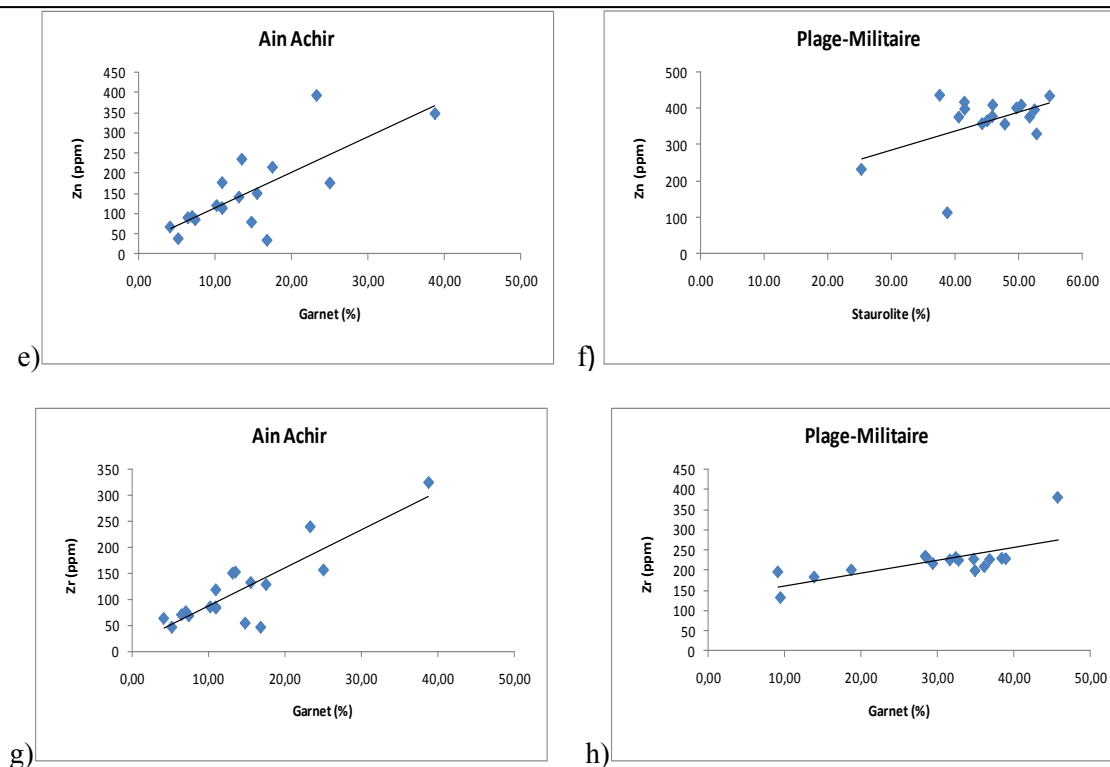


Figure.6. Correlation diagrams of traces element versus garnet and staurolite for Ain Achir and Plage-Militaire beach

## 5.2. Principal Component Analysis (PCA)

Geochemical factor analyses (PCA) aid the identification of parameters controlling chemical element and to interpret the relation between heavy mineral and chemical data [16, 17]. The trace element PCA data matrixes of the two beaches are shown in table 4. This table shows that the two first factors (F1 and F2) account for 79.56 % and for 81.01% of total variance at Ain Achir and Plage-Militaire beaches respectively, therefore in this study only these two first factors have been described.

At Ain Achir beaches, the table 4a show that the Factor 1 explains 62.70% of total variance. This factor is characterized by high loading of staurolite and garnet, all trace elements (excluding Ba and Sr) and REEs are on the positive side and kyanite, calcite, quartz, Ba, Sr and Ba are on the negative one. The traces element variables and the heavy minerals (garnet, staurolite) are highly associated with factor 1, therefore it can be interpreted as ferromagnesian mineral (staurolite–garnet) factor. Factor 2 explain about 16.86 % of variance and is characterized by high loading of tourmaline and Ba on the positive side and kyanite, calcite, quartz, Sr, Ni, and REE on the negative one. These allows us to interpret factor 2 (F2) as the non-ferromagnesian mineral factor. On the biplot F1 vs F2 (Fig.7a) it can be distinguish two groups: (i) one the positive side of F1 and F2 composed by the heavy mineral (garnet, staurolite, tourmaline), all the trace element –Sr, and the REEs and (ii) on the negative side of F1 and F2 plots the second group (kyanite, calcite, quartz and Sr). The biplot figure 7b confirms strongly the relationship between the garnet, staurolite and the traces-Sr and REE elements. It confirms also the relationship between Sr and the light minerals (calcite and quartz) which can be the source of this element.

Plage-Militaire: the table 4b shows that the factor Factor 1 (F1) accounted for 66.34% and factor 2 (F2) for 14.67%. Factor 2 (F2) explain 14.67% of the total variance. The positive right side of F2 is characterized by high loading of garnet and the REEs, whereas the negativ right side shows that staurolite is stongly associated to V, Y, Ni, Cr and Zn. The total variance of F1 and F2 (81.01) is higher than for Ain Achir (F1-F2=79.56%). The biplot (F1-F2) (Fig.7b) shows some similarities with the F1-F2 biplot of Ain Achir. In regard to F1 axis, it can be distinguish two groupes : the first one located on the positive side of the axis includes garnet, staurolite, REEs and the trace elements-Sr and Ba, and confirms the high relationship of these elements with the ferromagnesian phases (garnet and

staurolite) and a second one, on the negative side, composed by kyanite, tourmaline, quartz, calcite, epidote and the traces elements Sr and Ba. These latter elements have high affinity with non-ferromanesian minerals (i.e. quartz, calcite, tourmaline and kyanite).

Table 4. Mineral, Traces and REE variable eigen values for the first four factors: a) of Ain Achir, b) of the Plage-Militaire beaches

| a)                     | F1           | F2           | F3          | F4          |
|------------------------|--------------|--------------|-------------|-------------|
| <b>Variabilité (%)</b> | <b>62.70</b> | <b>16.86</b> | <b>5.44</b> | <b>4.75</b> |
| Grt                    | 0.11         | 0.33         | -0.10       | 0.14        |
| St                     | 0.14         | 0.16         | 0.18        | 0.49        |
| Ky                     | -0.10        | -0.12        | 0.27        | -0.27       |
| Tur                    | 0.01         | 0.25         | -0.32       | 0.20        |
| Ep                     | 0.00         | 0.01         | -0.48       | -0.05       |
| Qz                     | -0.10        | -0.30        | 0.02        | -0.25       |
| Cal                    | -0.13        | -0.25        | -0.02       | -0.43       |
| Ba                     | -0.08        | 0.20         | -0.38       | -0.20       |
| Cr                     | 0.20         | 0.17         | 0.00        | -0.21       |
| Ga                     | 0.20         | 0.15         | 0.08        | -0.16       |
| Nb                     | 0.13         | 0.30         | 0.01        | -0.28       |
| Ni                     | 0.14         | -0.01        | 0.50        | 0.06        |
| Sr                     | -0.15        | -0.23        | -0.25       | 0.07        |
| V                      | 0.20         | 0.16         | 0.13        | -0.14       |
| Y                      | 0.18         | 0.22         | 0.04        | -0.23       |
| Zn                     | 0.20         | 0.17         | 0.09        | -0.16       |
| Zr                     | 0.18         | 0.21         | -0.10       | -0.28       |
| La                     | 0.21         | -0.14        | -0.07       | -0.02       |
| Ce                     | 0.21         | -0.14        | -0.06       | 0.01        |
| Pr                     | 0.21         | -0.15        | -0.07       | 0.01        |
| Nd                     | 0.21         | -0.14        | -0.06       | 0.01        |
| Sm                     | 0.21         | -0.13        | -0.07       | 0.01        |
| Eu                     | 0.22         | -0.12        | -0.02       | -0.01       |
| Gd                     | 0.21         | -0.14        | -0.06       | 0.01        |
| Tb                     | 0.21         | -0.12        | -0.10       | 0.05        |
| Dy                     | 0.21         | -0.14        | -0.05       | 0.03        |
| Ho                     | 0.21         | -0.14        | -0.05       | 0.03        |
| Er                     | 0.21         | -0.13        | -0.05       | 0.03        |
| Tm                     | 0.21         | -0.13        | -0.03       | 0.02        |
| Yb                     | 0.21         | -0.13        | -0.05       | 0.03        |
| Lu                     | 0.22         | -0.12        | -0.06       | 0.03        |

| b)                     | F1           | F2           | F3          | F4          |
|------------------------|--------------|--------------|-------------|-------------|
| <b>Variabilité (%)</b> | <b>66.34</b> | <b>14.67</b> | <b>5.68</b> | <b>4.04</b> |
| Grt                    | 0.17         | 0.19         | 0.16        | 0.01        |
| St                     | 0.13         | -0.15        | -0.25       | -0.33       |
| Ky                     | -0.08        | -0.05        | 0.60        | 0.12        |
| Tur                    | -0.11        | -0.05        | -0.43       | 0.34        |
| Ep                     | -0.15        | 0.09         | 0.08        | 0.36        |
| Qz                     | -0.15        | -0.09        | 0.41        | 0.15        |
| Cal                    | -0.20        | -0.06        | 0.15        | -0.09       |
| Ba                     | -0.06        | 0.13         | -0.03       | 0.63        |
| Cr                     | 0.13         | -0.34        | -0.10       | 0.21        |
| Ga                     | 0.06         | 0.44         | -0.08       | 0.03        |
| Nb                     | 0.01         | 0.46         | -0.05       | -0.01       |
| Ni                     | 0.12         | -0.19        | 0.17        | 0.13        |
| Sr                     | -0.21        | -0.08        | -0.05       | -0.07       |
| V                      | 0.18         | -0.16        | -0.19       | 0.12        |
| Y                      | 0.22         | -0.06        | 0.11        | -0.01       |
| Zn                     | 0.10         | -0.39        | -0.13       | 0.21        |
| Zr                     | 0.12         | 0.38         | -0.08       | 0.08        |
| La                     | 0.22         | 0.02         | 0.00        | 0.10        |
| Ce                     | 0.22         | 0.01         | -0.01       | 0.08        |
| Pr                     | 0.22         | 0.02         | 0.01        | 0.09        |
| Nd                     | 0.22         | 0.02         | -0.02       | 0.08        |
| Sm                     | 0.22         | 0.01         | -0.01       | 0.05        |
| Eu                     | 0.21         | 0.03         | 0.00        | 0.14        |
| Gd                     | 0.22         | 0.01         | 0.05        | 0.03        |
| Tb                     | 0.22         | 0.00         | 0.06        | -0.04       |
| Dy                     | 0.22         | 0.01         | 0.09        | -0.03       |
| Ho                     | 0.22         | 0.00         | 0.08        | -0.04       |
| Er                     | 0.22         | 0.00         | 0.08        | -0.04       |
| Tm                     | 0.22         | 0.00         | 0.09        | -0.02       |
| Yb                     | 0.22         | -0.01        | 0.08        | -0.03       |
| Lu                     | 0.22         | 0.00         | 0.08        | -0.01       |

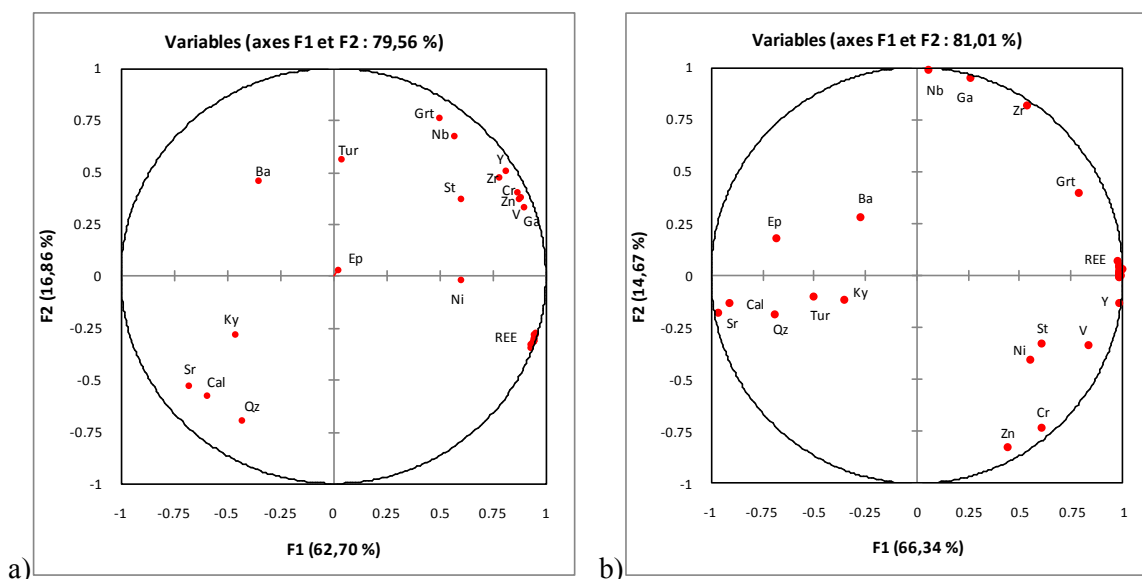


Figure.7. PCA biplot of the heavy minerals, traces and REE elements: a) at Ain Achir beach, b) at the Plage-Militaire beach.

## 6. CONCLUSION

The study of the elements distribution versus modal mineral composition, correlation matrix and the PCA circles has allowed us to conclude that there is a strong relationship between the amount of heavy minerals (garnet, staurolite) in the sand and the major, trace and REE elements. The trace elements (Ga, V, Zn, Ni, Cr, Y and Zr) are more related to garnet and staurolite, whereas the high concentrations of Sr and Ba are attributed to the presence of minerals: i.e. calcite, quartz, tourmaline and kyanite. From the light sand at Ain Achir to the dark one at Plage-Militaire, the REEs content increases with increasing the modal content in heavy minerals, especially in garnet and staurolite. The sand chemistry of the Ain Achir and the Plage-Militaire beach is controlled by their mineralogical composition.

## ACKNOWLEDGEMENTS

We are very grateful to anonymous reviewers for their helpful comments and suggestions that improved this manuscript. Moreover, we thank the Institute of Earth and Environmental Science, University of Potsdam for their support in analytical facilities and the Department of Mining/Badji-Mokhtar University for their support in sample preparation.

## REFERENCES

- [1] Hadj Zobir S., Altenberger U. & Günter C., 2017. The Edough Massif garnetites: evidences for a metamorphosed paleo-garnet beach-sand placer (Cap de Garde, Annaba, Northeast Algeria), *Journal of Mediterranean Earth Sciences*, Vol.9, 1-13
- [2] Hadj Zobir S., Altenberger U. & Günter C., 2014. Geochemistry and petrology of metamorphosed submarine basic ashes in the Edough Massif (Cap de Garde, Annaba, northeastern Algeria), *Comptes Rendus Géoscience* 346, 244-254 .
- [3] Brunnel M., Hammor D., Misseri M., Gleizes G. & Bouleton J., 1988. Cisaillements synmétamorphes avec transport vers le Nord-Ouest dans le massif cristallin de l'Edough (Est Algérien), *Comptes Rendus Géoscience* 306, 1039-1045.
- [4] Ahmed-Said Y., Leake B.E. & Rogers G., 1993. The petrology, geochemistry and petrogenesis of the Edough igneous rocks, Annaba, NE Algeria, *Journal of African Earth Sciences*, Vol. 17 (1), 111-123.
- [5] Ahmed-Said Y. & Leake B.E., 1995. The petrogenesis of the Edough orthogneisses, Annaba, northeast Algeria, *Journal of African Earth Sciences*, Vol.21, 253-269.
- [6] Caby R. & Hammor D., 1992. Le Massif cristallin de l'Edough (Algérie): un " Métamorphic Core Complex" d'âge miocène dans les Magrèbides, *Comptes Rendus Géoscience* 314, 829-835.
- [7] Caby R., Hammor D. & Delor C., 2001. Metamorphic evolution, partial melting and Miocene exhumation of lower crust in the Edough metamorphic core complex, west Mediterranean orogen, eastern Algeria, *Tectonophysics* 342, 239-273.
- [8] Darnley AG., Bjorklund A., Bolviken B., Gustavsson N., Koval PV., Plant J.A., Steenfel A., Tauchid M & Xie X., 1995. A Global Geochemical Database for Environmental and Resource Management, Recommendations for International Geochemical Mapping. Final report of IGCP project 259. UNESCO Publishing.
- [9] Whitney D.L. & Evans B.W., 2010. Abbreviations for names of rock-forming minerals, *American Mineralogist*, Vol. 95 (1), 185-187
- [10] Rothwell R.G., 1989. *Minerals and Mineraloids in Marine Sediments: an Optical Identification Guide*. London: Elsevier.
- [11] Rudnick R.L. & Fountain D.M., 199. Nature and composition of the continental crust -- a lower crustal perspective. *Reviews of Geophysics* Vol.33, 267-309.
- [12] Rudnick R.L. & Gao C., 2005. Composition of the continental crust; in R.L. Rudnick, ed., *The Crust: Treatise on Geochemistry*, Vol. 3, Elsevier, San Diego, California, 1-64
- [13] Samson I.M. & Wood S., 2005. The rare-earth elements: behavior in hydrothermal fluids and concentration in hydrothermal mineral deposits, exclusive of alkaline settings; in Linnen, RL and Samson, IM eds., *Rare-element geochemistry and mineral deposits*, Geological Association of Canada, GAC Short Course Notes, Vol.17, 269-297
- [14] Castor S.B. & Hedrick L.B., 2006. Rare earth elements; in Kogel, J.E, Trivedi, N.C., Barker, J.M., and Krukowski, S.T., ed., *Industrial Minerals volume*, 7th edition: Society for Mining, Metallurgy, and Exploration, Littleton, Colorado, 769-792.
- [15] Monecke T., Kempe U. & Götz J., 2002. Genetic significance of the trace element content in metamorphic and hydrothermal quartz: A reconnaissance study, *Earth and Planetary Science Letters*, Vol. 202, p. 709-724.
- [16] Pirkle F.L., Pirkle E.E., Pirkle A. & Dicks S.E., 1985. Evaluation through correlation and principal component analyses of delta origin for the Hawthorne and Citronelle sediments of peninsular Florida. *Journal of Geology*, Vol.93, 493-501
- [17] Svendsen J.B., 2002. *Sedimentology and High-Resolution Stratigraphy of Fluvial-Aeolian Sequences Using Integrated Elemental Whole Rock Geochemistry*. Ph.D.thesis, University of Aarhus, Denmark.